Electromagnetic Diagnosis of First Stage Breast Cancer

ISMAEEL M. AWAD, German University in Cairo, Egypt
AYA M. HAKIK, German University in Cairo, Egypt
MOHAMAD H. M. HASSANIN, German University in Cairo, Egypt
PIERRE LOUKA, German University in Cairo, Egypt
MAZEN NABIL DESOUKY, German University in Cairo, Egypt
PROF. DR. A. M. M. A. ALLAM, German University in Cairo, Egypt

In this paper, a spiral rectangular antenna is designed and implemented for human first stage breast cancer diagnosis. It is optimized to operate in the Industrial, Scientific, and Medical (ISM, 2.4–2.5 GHz) band. It achieves a reflection coefficient less than −10 dB in air. The breast model is constructed using five tissues: skin, fat, fibro-glandular, muscle and lymph nodes for a healthy body. The antenna is implanted on the breast model and investigated for different stages of tumor sizes and locations. All tumor locations and sizes were found to cause a significant change in the resonance frequency.

CCS Concepts: • **Hardware** → *Sensors and actuators*; • **Applied computing** → **Engineering**; **Imaging**.

Additional Key Words and Phrases: breast cancer, spiral antenna, first stage, modified phantom

ACM Reference Format:
Ismaeel M. Awad, Aya M. Hakik, Mohamad H. M. Hassanin, Pierre Louka, Mazen Nabil Desouky, and Prof. Dr. A. M. M. A. Allam. 2025. Electromagnetic Diagnosis of First Stage Breast Cancer. In *Proceedings of 2025 8th International Conference on Digital Medicine and Image Processing (DMIP '25).* ACM, New York, NY, USA, 9 pages. https://doi.org/10.1145/3785443.3785449

1 INTRODUCTION

One of the largest global health issues is cancer, which resulted in over 20 million new cases and 9.7 million deaths worldwide in 2022 [10]. Lung, breast, and colorectal cancers are the most prevalent forms and account for a significant portion of the global health burden. In particular, breast cancer is the most common type of cancer diagnosed in women; in 2022, it was responsible for over 670,000 deaths worldwide and more than 2.3 million new cases. More research is required to improve early breast cancer detection, as it greatly increases treatment success. Continuous monitoring is also needed to track recurrence, making electromagnetic antenna systems a promising solution.

For oral cancer, [6, 7] diagnosed it using spiral patch antennas in the MICS and ISM bands. To obtain a realistic simulation of the breast, electrical conductivity and permittivity values of the breast tissues were included to achieve an accurate simulation. These parameters were taken from earlier researches [11]. An obvious dielectric contrast between

Authors' addresses: Ismaeel M. Awad, ismaeel.awad@student.guc.edu.eg, German University in Cairo, Cairo, Egypt; Aya M. Hakik, aya.aly@student.guc.edu.eg, German University in Cairo, Cairo, Egypt; Mohamad H. M. Hassanin, mohamad.hassanin@student.guc.edu.eg, German University in Cairo, Cairo, Egypt; Pierre Louka, pierre.louka@student.guc.edu.eg, German University in Cairo, Cairo, Egypt; Mazen Nabil Desouky, mazin.desouky@student.guc.edu.eg, German University in Cairo, Cairo, Egypt; Prof. Dr. A. M. M. A. Allam, abdelmegid.allam@guc.edu.eg, German University in Cairo, Cairo, Egypt.

Table 1. Dimensions of the Antenna in Air

Parameter	GW	GH	P1W	P1L	P2W	P2L	P3W	P3L
Value (mm)	20	20	15	4	3.2	11	11.8	2.4
Parameter	**P4W**	**P4L**	**P5W**	**P5L**	**FP**	**SP**		
Value (mm)	1.6	7.95	5	0.8	13.5	12.5		

malignant and healthy tissues is included. In [9], a 4×4 antenna array was designed to work at 8 GHz. A square patch antenna was created in [5] to resonate within the ISM band. [12] implemented a square slotted patch antenna with a modified ground plane to resonate within the ISM band. In [2], a microstrip patch antenna with a truncated ground was simulated and manufactured, lymph nodes were also included in the simulation. E. Hanafy and A. Allam (2014) have developed spiral patch antennas to detect breast cancer in both the ISM and MICS bands [3, 4]. Another study [1] diagnosed stage II cancer in a hemispherical breast model including lymph nodes.

The current study expands on this by including the function of lymph nodes and other structures. Building on recent insights, this approach seeks to provide a more biologically realistic representation of the breast for improved detection and monitoring. The paper is organized as follows: section II presents the design, in section III discusses results, and section IV concludes.

2 DESIGN

This section presents the design of the antenna and breast phantom followed by the design methodology.

2.1 Antenna Design

Fig. 1 and Fig. 2 show the rectangular printed spiral planar antenna developed for this work [4]. The design targets operation in the ISM band of 2.4–2.5 GHz. The aim is achieving good impedance matching (S_{11}). For this paper, a spiral planar rectangular antenna is used. It is selected because of its compact size and simple fabrication process, which make it appropriate for biomedical use [11].

The ground plane, patch, and coaxial feed are implemented using annealed copper with a conductivity of 5.8×10^7 $^{S}/_{m}$ and a density of 8930 $^{kg}/_{m^3}$. The substrate is made of Rogers 4350B with a relative permittivity of 3.66 and a conductivity of 0.0037 $^{S}/_{m}$. The height of the substrate is 1.524 mm. To enhance stability and offer protection, a superstrate layer of identical material and thickness is added. The 50 Ω coaxial feed is designed with an inner diameter of 0.482 mm, outer diameter of 1.614 mm and outer copper thickness of 0.05 mm. The dielectric material used in the coaxial feed is PTFE with a relative permittivity of 2.1, a conductivity of 0.0002 $^{S}/_{m}$, and a density of 2200 $^{kg}/_{m^3}$. The missing dimensions of the structure are depicted in Table 1.

2.2 Breast Phantom Design

A simplified breast phantom is modeled by a hemisphere of radius 75 mm as depicted in Fig. 3. It contains three different layers; skin, fat, and muscle. Fibro-glandular tissues and lymph nodes are included in the fat layer as a modification for the breast model. Three lymph nodes were modeled on either side of the fibro-glandular tissue as spheres with radii of 7.5 mm [8], and a duct is added with a radius of 0.5 mm on each side. The thickness of skin, fat and muscle are 0.7 mm, 85.5 mm, and 25 mm respectively. The properties of all these materials are presented in Table 2. The 3D view of the

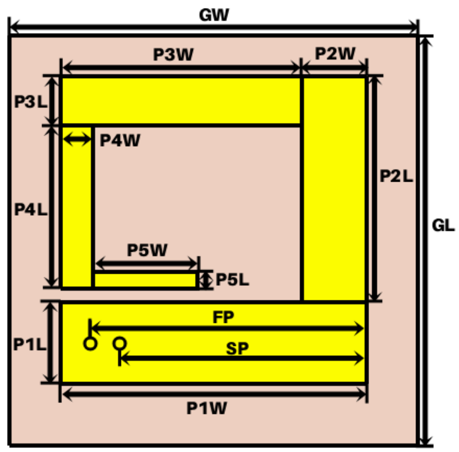

Fig. 1. Antenna design in air

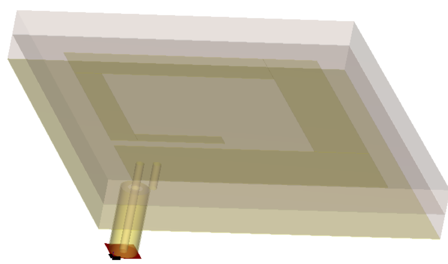

Fig. 2. 3D view of the antenna and coaxial Feed

Table 2. Properties of Materials

Tissue	ε_r	σ ($^{S}/_{m}$)	ρ ($^{kg}/_{m^3}$)
Skin	37.9735	1.478	1100
Fat	5.14085	0.139	920
Fibro-glandular	57.2	1.99	1050
Muscle	52.668	1.773	1060
Lymph Node	78	0.965	1050
Tumor	46.1	0.68	1050

breast is illustrated in Fig. 4. For the sake of mounting the antenna sensor on the top of the breast, the area of the nipple is flattened with a suitable area of approximately 530.929 mm^3 to fit the antenna as shown in Fig. 4a.

The methodology of this research is as follows: the antenna is placed in direct contact with the surface of the phantom and positioned vertically, similar to the placement of a stethoscope as shown in Fig. 4a. It is optimized to resonate within the ISM band for a healthy body. The length of the arm, P5W, is changed to 0.7 mm to compensate for the

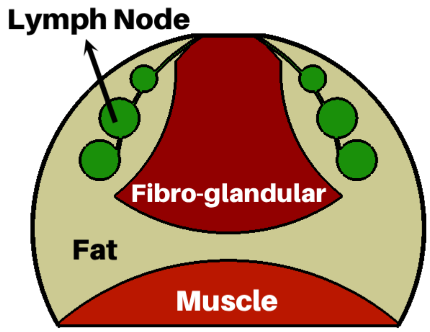

Fig. 3. Cross-sectional view of breast phantom

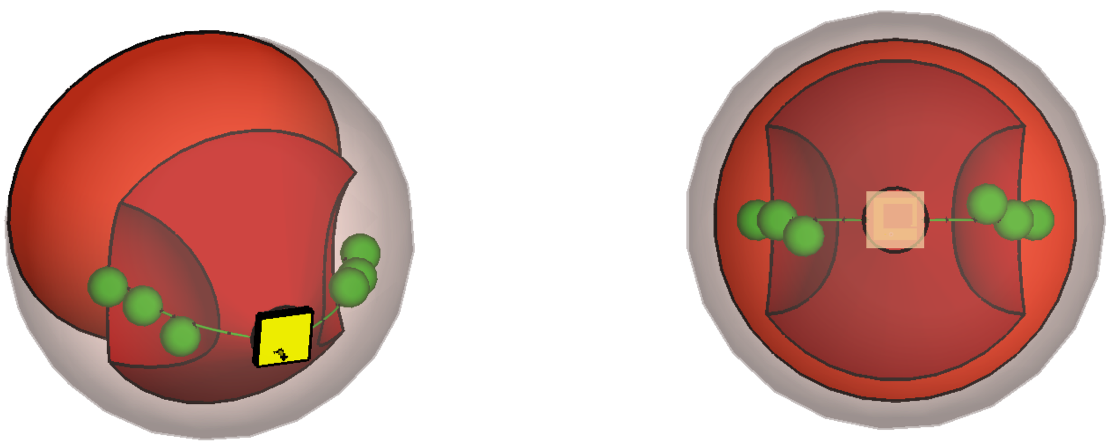

(a) Isometric view

(b) Front view

Fig. 4. 3D views of breast phantom with mounted antenna

frequency shift. Moreover, the position of the coaxial feed and shorting pin, FP and SP, were changed to 6 mm and 4 mm, respectively, to improve matching.

To mimic early-stage breast cancer, tumors were introduced in different positions within the fibro- glandular region and the lymph nodes. In the lymph nodes, the tumors were always arranged in clusters of three to reflect typical patterns of metastatic spread.

Several scenarios were examined. In the simplest case representing stage IA, a single tumor is placed in the fibro-glandular tissue as shown in Fig. 5. Subsequent cases representing stage IB considered one tumor in the fibro-gland along with tumors in two lymph nodes, then tumors distributed in four lymph nodes, followed by four nodes with an additional fibro-gland tumor. Finally, arrangements involving six lymph nodes alone and six nodes with a fibro-gland tumor were analyzed. These cases were intended to replicate clinically relevant patterns of tumor growth.

Then, the reflection coefficient (S_{11}) is calculated for each case and compared against the healthy breast model. Shifts in resonance frequency and changes in impedance matching were carefully examined. As illustrated in Fig.

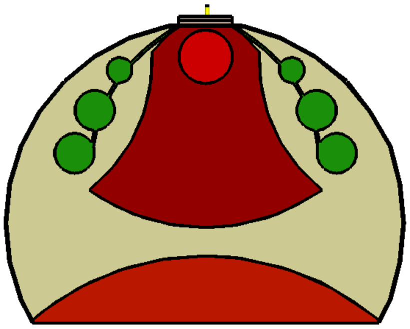

(a) Cross-sectional view

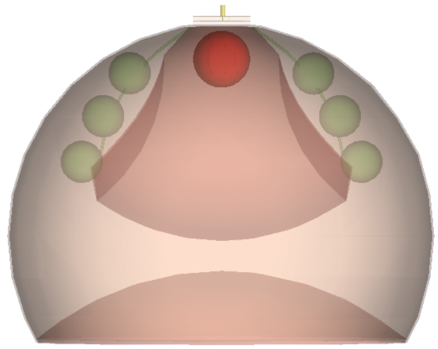

(b) 3D view

Fig. 5. Stage IA

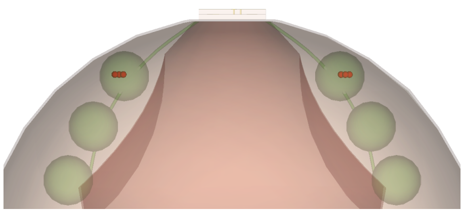

(a) 2 groups

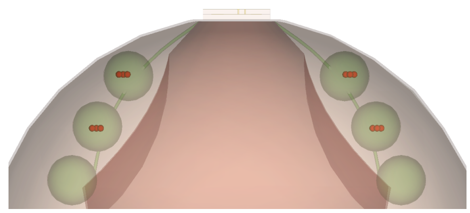

(b) 4 groups

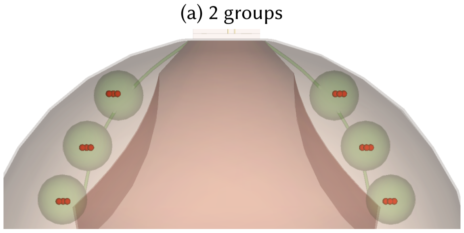

(c) 6 groups

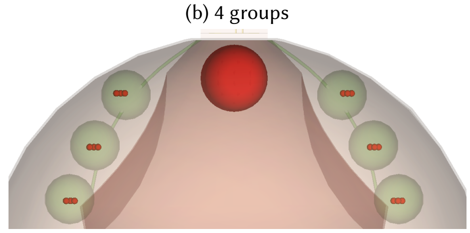

(d) 6 groups with fibro-glandular Tumor

Fig. 6. Stage IB

11, increasing the number of tumors generally caused the resonance frequency to shift upward and the return loss magnitude to decrease. The frequency variation remained modest, however, due to limited wave penetration into tissues at this frequency band.

3 RESULTS

The antenna shown in Fig. 1 was fabricated and measured using a Vector Network Analyzer as shown in Fig. 7. The simulated and measured reflection coefficient for the antenna in air is shown in Fig. 8, with the simulation producing a minimum of -17.54 dB at a frequency within the standard ISM band. This is well below the standard -10 dB and shows good matching. The difference in resonant frequencies between the measured and simulated antennas was considered negligible for the purposes of this paper and could be improved in future works.

(a) The spiral design of the antenna

(b) The antenna with the superstrate layer

Fig. 7. The antenna designed to work in air being measured

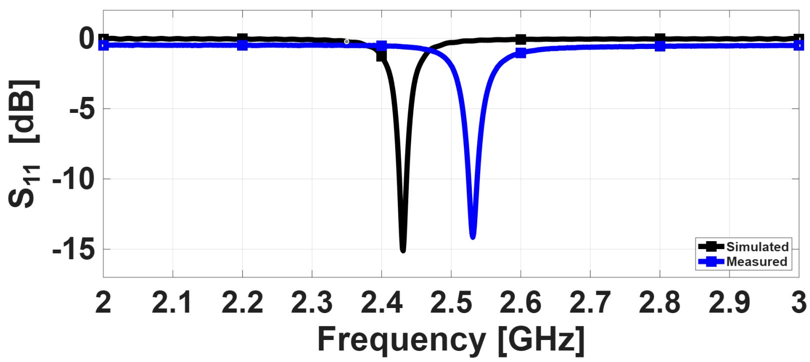

Fig. 8. Comparison of simulated and measured S_{11} of antenna in air

Once the antenna is implanted on the breast, the Specific Absorption Rate (SAR) of the breast is measured at a frequency of 2.45 GHz (the median frequency) averaged over 10 grams. The absolute maximum SAR reached is 0.585 W/kg in the region closest to the antenna placement as shown in Fig. 9. This is below the allowed maximum localized SAR according to the IEEE standard.

Fig. 10 shows the reflection coefficient in the range of 2.4 to 2.5 GHz when implanted in a healthy breast and the stage IA tumor-containing breast (a single large tumor near the fibro-glandular tissue). The graph indicates that the presence of the tumor caused the resonance frequency of the antenna to decrease noticeably from 2.4500 healthy breast to 2.4470 GHz, a shift of 3 MHz.

Fig. 11 shows the reflection coefficient obtained for stage IB breast cancer with 2 groups, 4 groups, and 6 groups of tumors in lymph nodes with and without the fibro-glandular tissue tumor, respectively, compared to healthy breast. The resonance frequencies for all cancerous breasts are consistently lower than those of a healthy breast. The resonant frequencies without gland tumors were 2.4480 GHz, 2.4410 GHz, 2.4400 GHz for 2 groups, 4 groups, and 6 groups, respectively. With gland tumors, the frequencies are 2.4450 GHz for 2 and 4 groups and 2.4440 GHz for 6 groups. All shifts are above 2 MHz. Table 3 summarizes the frequency shift for all scenarios adopted in this work.

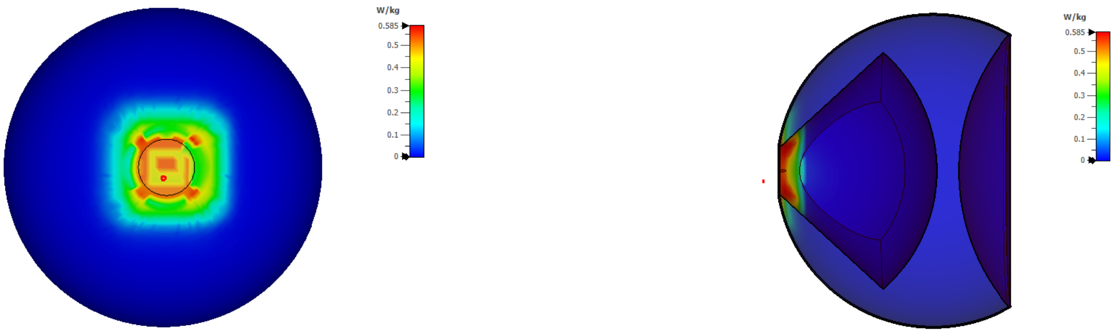

(a) Front view (b) Cross-sectional view

Fig. 9. SAR results

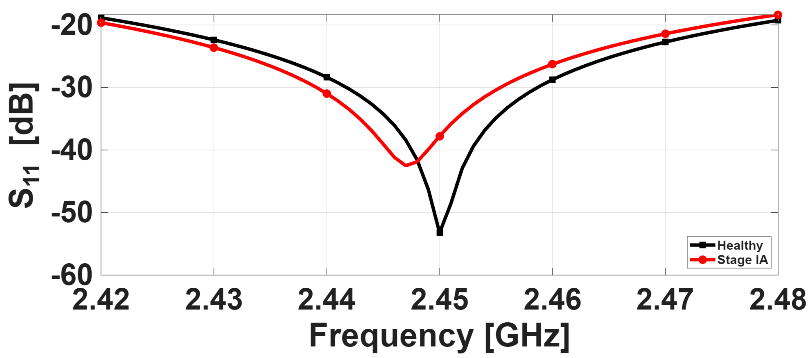

Fig. 10. Stage IA

Table 3. Frequency Shift Caused by Tumors

No. of Groups in Lymph Nodes	**2**	**4**	**6**
Frequency Shift without Gland Tumor (MHz)	2	9	10
Frequency Shift with Gland Tumor (MHz)	5	5	6

These results may still be different from a physical measurement as specific tissnues such as mammary glands and ducts were not modelled or differentiated from the fibrous tissue. This could lead to some discrepancy between simulated and measured results in some cases.

4 CONCLUSION

In this paper, a model for the human breast is implemented. An antenna operating in the Industrial, Scientific and Medical (ISM) band is designed and implemented on CST Microwave Studio. The first stage of human breast cancer is investigated using different sizes and locations in the glands and lymph nodes. It is found that the different locations and sizes of the tumors have a significant effect on the resonance of the implanted antenna.

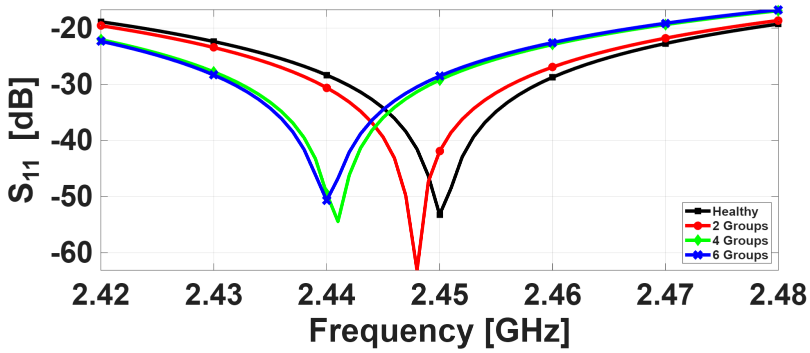

(a) Tumor in lymph nodes only

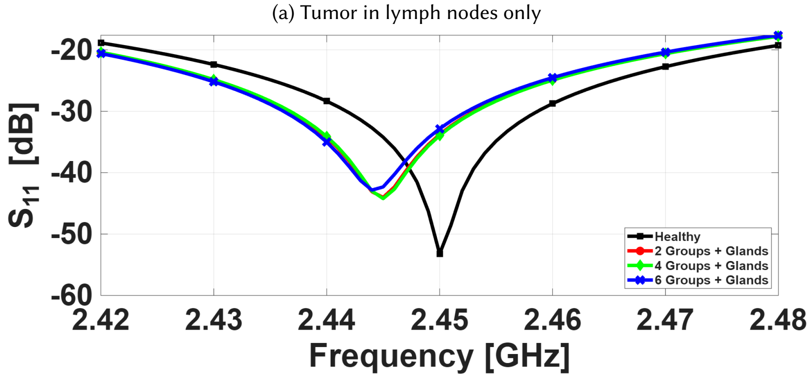

(b) Tumor in lymph nodes and glands

Fig. 11. Stage IB

REFERENCES

[1] N. Ali, M.F. Abo Sree, R. Uyguroglu, and A.M.M.A. Allam. 2020. Stage II cancer diagnosis using printed antenna implemented on hemispherical model for human breast. *Journal of Instrumentation* 15, 09 (sep 2020), P09016. https://doi.org/10.1088/1748-0221/15/09/P09016

[2] Nagia Ali, Rasime Uyguroglu, and Abdelmegid Allam. 2018. Cancer Diagnosis in Breast Using Biological and Electromagnetic Properties of Breast Tissues on Antenna Performance. 325–329. https://doi.org/10.1109/MMS.2018.8612104

[3] Engy Alaa El Din Hanafy and Abdelmegid Allam. 2014. Diagnosis of Breast Tumors using a PIFA antenna. *International Journal of Computer and Information Technology* 03 (2014).

[4] Engy Alaa El Din Hanafy and Abdelmegid Allam. 2014. Investigation for breast cancer using antennas in the ISM frequency band. In *2014 IEEE Conference on Antenna Measurements & Applications (CAMA)*. 1–3. https://doi.org/10.1109/CAMA.2014.7003416

[5] Mussa Elsaadi, Hend Muhmed, Mohammed Alraheem, Hajir Miftah, and Omar Salah. 2019. Square Patch Antenna for Breast Cancer Diagnosis at 2.45 GHz. *Circuits and Systems* 10 (01 2019), 45–53. https://doi.org/10.4236/cs.2019.104004

[6] Omar Hammouda. 2014. Utilizing Implanted Antennas to Detect the Presence of Oral Cancers. *Research Journal of Engineering Sciences, 2278-9472* 3 (07 2014), 22–27.

[7] Omar Hammouda and Prof Allam. 2014. DIAGNOSIS OF ORAL CANCERS USING IMPLANTED ANTENNAS.

[8] H.L. Ioachim and L.J. Medeiros. 2009. *Ioachim's Lymph Node Pathology.* Wolters Kluwer Health/Lippincott Williams & Wilkins. https://books.google.com.eg/books?id=-hmfiFfdNbwC

[9] Fatma Mostafa, Michael Nasief, and Hala Mansour. 2019. 4*4 Micro strip Patch Antenna Array used to Breast Cancer Detection System. *Engineering Research Journal (Shoubra)* 1 (10 2019), 74–81. https://doi.org/10.21608/erjsh.2019.406491

[10] WHO. 2024. Global cancer burden growing, amidst mounting need for services — who.int. https://www.who.int/news/item/01-02-2024-global-cancer-burden-growing--amidst-mounting-need-for-services.

[11] Yera Yera, Jaehoon Kim, and Yoesoep Rachmad. 2006. *Implanted Antennas in Medical Wireless Communications.* Vol. 1. Morgan & Claypool Publishers. https://doi.org/10.2200/S00024ED1V01Y200605ANT001

[12] Rabia Çalışkan, S. Sinan Gültekin, Dilek Uzer, and Özgür Dündar. 2015. A Microstrip Patch Antenna Design for Breast Cancer Detection. *Procedia - Social and Behavioral Sciences* 195 (2015), 2905–2911. https://doi.org/10.1016/j.sbspro.2015.06.418 World Conference on Technology, Innovation and Entrepreneurship.

Received 21 September 2025; accepted 10 October 2025